Summary: Hydrogenated nanocrystalline silicon (nc-Si:H) was deposited by plasma-enhanced chemical vapor deposition (PECVD) on transparent polymers in order to qualify these for possible use as electronic substrates. As a first step, plasma etch experiments in pure H_2 revealed small etch rates for these materials. Thin films of nc-Si:H were then deposited on samples placed on the grounded electrode of a "Reinberg"-type parallel plate RF (13.56 MHz) PECVD reactor, at various substrate temperatures ($25\,°C \leq Ts \leq 250\,°C$), using SiH_4 diluted in H_2 as the feed-gas. Thermally induced failure of the nc-Si:H/polymer composite was avoided within a certain range of deposition conditions, permitting structural and electrical characterization of the deposits.

Temperature-dependent conductivity, $\sigma(T)$, for nanocrystalline silicon (nc-Si:H) films on glass and three polymer substrates, all deposited at $T_s = 175\,°C$.
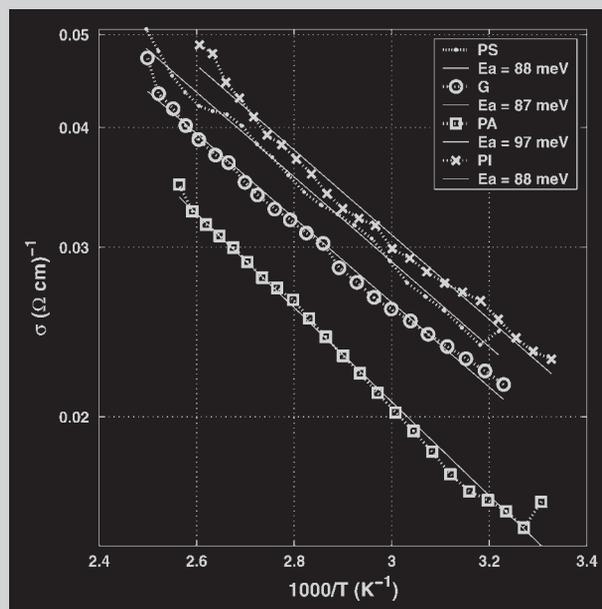
PECVD of Nanocrystalline Si Layers on High-T_g Polymer Substrates

Luke A. MacQueen,[1] *Janik Zikovsky,*[1] *Gilles Dennler,*[2] *Mohamed Latreche,*[3] *Grzegorz Czeremuszkin,*[3] *Michael R. Wertheimer**[1]

[1] Groupe des Couches Minces and Department of Engineering Physics, École Polytechnique, Montréal, QC, Canada
Fax: 001 514 340 3218; E-mail: michel.wertheimer@polymtl.ca
[2] Linz Institute for Organic Solar Cells (LIOS), Johannes Kepler University, Linz, Austria
[3] Nova-Plasma Inc., Montréal, QC, Canada

Introduction

Electronic devices on flexible polymer substrates are becoming increasingly important, for example in displays, photovoltaic cells, etc. The advantages of using polymer substrates instead of glass for electronic applications include light weight, flexibility and conformability, and low cost with the possibility of roll-to-roll processing (large-area electronics). So far, the adoption of polymers for electronic applications has been slow due to their limited compatibility with semiconductor fabrication processes. In particular, the relatively high linear expansion coefficient, α, and low glass transition temperature, T_g, of most polymers limit their use to temperatures below 300 °C. Several high-T_g polymers ($220\,°C < T_g < 330\,°C$) with optical transparency, good chemical resistance and barrier properties have recently been developed for use in organic (OLED) display technology,[1,2] and these have motivated the present research.

For many applications, thin film transistor (TFT) matrix arrays are required, for example to drive the individual pixel elements of a display.[3,4] Hydrogenated amorphous silicon (a-Si:H) is a low-temperature material which is presently used as a TFT semiconductor, but its inherently low charge

carrier mobility limits the density at which TFTs can be laid out. Better nano-structural control of low-temperature Si films is therefore required to increase TFT density and to reduce operating power of TFT-based devices. Silicon can be deposited as various structural phases ranging between a-Si and the fully crystalline state (c-Si); these include nanocrystalline (nc-Si), microcrystalline (μc-Si), and poly-crystalline (pc-Si) materials. The first two (nc-Si and μc-Si) comprise an a-Si matrix in which are dispersed many tiny crystallites (small volumes of c-Si), the "nano" and "micro" prefixes indicating the mean crystal size. Pc-Si refers to a material that is devoid of the amorphous matrix, the crystallites being separated by abrupt grain boundaries. Although c-Si and pc-Si possess high carrier mobility in comparison to a-Si, they are brittle and in-flexible, unlike a-Si. Furthermore, as transistor dimensions are reduced, conductivity anisotropy within the pc-Si material becomes problematic.

Nanocrystalline silicon (nc-Si:H) is a preferred semi-conductor for fabricating TFTs, and deposition by plasma-enhanced chemical vapor deposition (PECVD) is partic-ularly advantageous when using temperature-sensitive substrate materials. With PECVD, the crystalline volume fraction of as-deposited Si films can be varied between 0 and close to 100% within a useful range of "low" substrate temperatures, T_s,[5−7] eliminating the requirement of post-deposition laser or thermal annealing. The objective of the present research has, therefore, been to deposit nc-Si:H films at the lowest possible T_s values, and to characterize their structural and electrical properties. No coatings were deposited before or after the nc-Si:H, which was deposited directly on the various substrates in order to simplify the estimation of stress values induced within the film-substrate (f-s) structure. Such stress values, resulting from differ-ential thermal expansion, α, can be correlated with results of structural and electrical measurements. In order to reduce possible contamination of the nc-Si:H by unwanted "dopant" elements (C, O, N, etc) arising from substrate ablation (etching) during PECVD, we first performed etching experiments in order to identify the optimal conditions for high-quality nc-Si:H film growth.
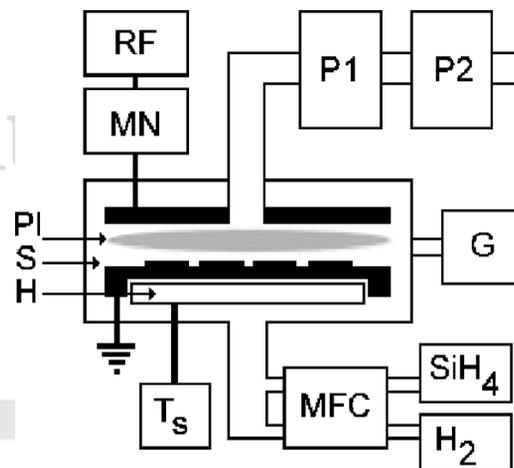

Figure 1. Schematic of RF-PECVD system: RF: 13.56 MHz Power Supply; MN: Matching Network; P1: Turbo Molecular Pump; P2: Rotary Pump; G: Pressure Gauge; T_s: Temperature Control; MFC: Mass Flow Control; Pl: Plasma; S: Substrates; H: Heater.

Experimental Part

Etching and Deposition Experiments

Etching and deposition experiments were performed in a "Reinberg-type" parallel-plate RF-PECVD reactor, operating at 13.56 MHz (Figure 1). The ranges of operating parameters selected and the reasons for these choices will be clarified later in this text. The substrate materials used in this research and some of their key properties for this work (α and T_g) are presented in Table 1. Since nc-Si:H films must not be contaminated by unwanted impurities, the polymer substrates must be resistant towards ablation (etching) in H_2-rich plasma during the PECVD process. It was, therefore, deemed necessary to investigate possible etching of the polymer substrates as a preliminary step. Etch rates were determined by partially masking the substrates with 50 nm Au layers before exposing them to H_2 plasma at various RF power densities (50 mW/cm² < P < 500 mW/cm²), and then profiling the etched areas by Atomic Force Microscopy (AFM). Such experiments were carried out with the substrates on the

Table 1. Properties of the substrate materials investigated.

Substrate	Source/Manufacturer[2]	Symbol	T_g (°C)	α
				ppm/°C[a]
APPEAR® (cyclic polyolefin)	Promerus LLC	PO	330	60 + T/4
ARYLITE® (polyarylate)	Ferrania Imaging Technologies.	PA	325	50 + T/15
SUMILITE® [poly(ether sulfone)]	Sumitomo Bakelite Co. Ltd.	PS	223	50 + T/14
KAPTON® (polyimide)	DuPont de Nemours & Co.	PI	360	20
Glass (Corning 2947)	Corning Inc.	G	–	9

a) T-dependent α values are linear approximations of data from ref.[1]

grounded or powered electrodes. The above-noted variation in P was then repeated, this time with a certain fixed concentration, C_{SiH_4}, of SiH_4 added to the H_2 (SiH_4 concentration, $C_{SiH_4} = [SiH_4]/([SiH_4] + [H_2]) = 6.25\%$). The resulting a-Si:H films were used for comparing deposition rates to etch rates.

In the case of nc-Si:H deposition experiments, P was maintained at 50 mW/cm^2, with substrates placed on the grounded electrode only. The SiH_4 and H_2 partial pressures were maintained constant at 8 mTorr and 120 mTorr, respectively ($C_{SiH_4} = 6.25\%$), the chamber pressure was always $p = 150$ mTorr (20 Pa), while the substrate temperature, T_s, was varied between 25 °C and 250 °C. Typical deposition durations were 200 min, and film thicknesses, d_f, measured by variable angle spectroscopic ellipsometry (VASE, J. Woollam & Co.), were 120 ± 15 nm.

Differential Thermal Expansion

The maximum value of T_s at which we could deposit nc-Si:H films on the substrates listed in Table 1 was mainly limited by the differences in thermal expansion coefficients, α, of the deposited Si films, α_f, and the substrates, α_s (see Figure 2 and Table 1). Substrates were heated ($dT_s/dt \approx 1$ °C/min) and held at the selected value of T_s for 30 min prior to film deposition. Precautions were taken to limit the amount of structural relaxation (for example, buckling or rolling) of the film-substrate (f-s) composite during deposition, and the PECVD chamber was gradually returned to ambient conditions ($dT_s/dt \approx -1$ °C/min) after the deposition had terminated. The differential thermal strain between the substrates and the film deposits can be approximated by

$$\delta = (\alpha_s - \alpha_f)\Delta T, \tag{1}$$

where α_s and α_f are the respective coefficients of thermal expansion. The thicknesses, d_f, of our nc-Si:H deposits were typically at least a thousand times less than those of the substrates. When $d_s/d_f \approx 10^3$ such as in the present case, curvature of the f-s composite resulting from stress relaxation may be expected to obey the Stoney formula up to $Y_f/Y_s \approx 100$, where Y is Young's modulus;[8] in the present case $Y_f \approx 150$–200 GPa[9] and $1.9 < Y_s < 5$ GPa.[1] Since $d_s Y_s/d_f Y_f > 10$, we can use the

following expression to estimate the compressive stress in the film due to differential thermal contraction:[10]

$$s_f = \frac{Y_f \delta}{(1 - v_f)} \tag{2}$$

where v_f is Poisson's ratio of nc-Si:H. Films deposited on PO, the polymer with by far the highest α_s value (see Figure 2 and Table 1), were observed to delaminate at $T_s \geq 200$ °C; in this particular case, the compressive strain $\alpha_s \Delta T \approx 1.7\%$ resulted in a stress $s_f \approx 3.6$ GPa, a value that clearly exceeded the f-s interfacial adhesion strength. These may, therefore, be considered the limiting conditions for successful deposition of stable nc-Si:H film coatings.

Physico-Chemical Characterization of Si Deposits

Thin Si deposits were subjected to both structural and electrical characterizations, primarily by micro-Raman spectroscopy (MRS) and by DC conductivity measurements, respectively. MRS was used to estimate the crystalline volume fractions, X_c, of the films by comparing the areas under Raman peaks corresponding to the crystalline (c) and amorphous (a) transverse optical lattice vibrations (c-TO and a-TO).[11–17] We used an argon-ion laser, $\lambda = 514$ nm, in the Stokes configuration, and calibrated the measured spectra with a c-Si sample displaying a c-TO peak centered at 520.5 cm^{-1} with a full width at half-maximum (FWHM) of 3.886 cm^{-1}. Data analysis (spectral deconvolution and area integration) was done using BOMEM GRAMS/32 software (Galactic Industries Co., Salem, NH).

DC conductivity measurements were performed by the four-point-probe method,[18] with samples mounted on a temperature-controlled substrate holder and using computerized data acquisition. This system, that allowed us to measure sheet conductivity during repeated thermal cycling, comprised a Keithley 220 programmable current source, an Agilent 34401A multimeter, and a Temptronic temperature controller; probe tip spacings and radii were 1.59 mm and 17.8 μm, respectively. For the case of very low conductivity samples ($\sigma < 10^{-6}$ S/cm), planar aluminum electrodes (with a 100 μm gap) were evaporated on the Si films, and measurements were carried out under vacuum.

Results and Discussion

Etching and Deposition Experiments

Figure 3 presents etch rates, E, of three of the present polymers in pure H_2 plasma, samples being placed either on the grounded or the powered electrodes. Significantly higher etch rates are seen to occur on the powered electrode ($P < 0$, in Figure 3) on account of d.c.-bias induced ion bombardment.[19] E values were very small for the case of low power densities ($|P| < 50$ mW/cm^2), especially in the absence of energetic ion bombardment, on the grounded electrode. Figure 4 presents the influence of P on the deposition rate, D, and the refractive index, n, of a-Si:H films, deposited at $T_s = 27$ °C on glass. Dense films (high
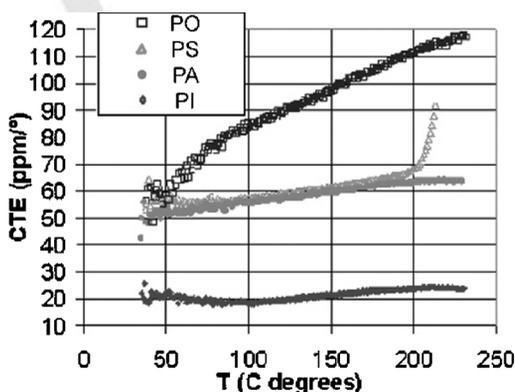

Figure 2. Coefficient of thermal expansion, α, (ppm/°) of four high-T_g polymers versus T. From ref.,[1] with permission.
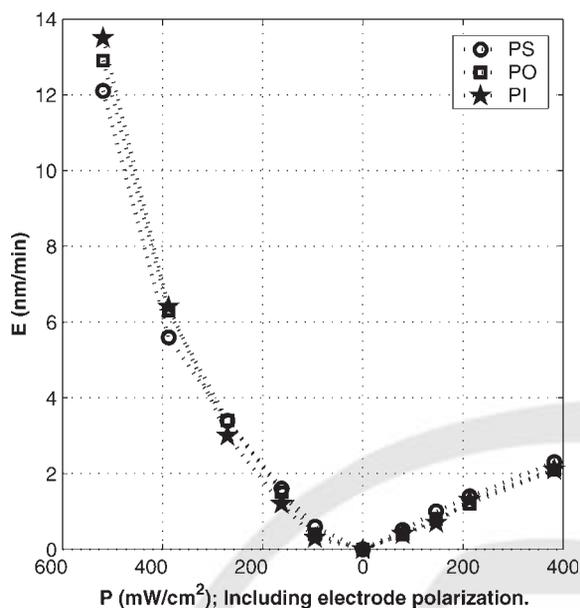
Figure 3. Etch rates, E, for three of the high-T_g polymers, as a function of power density, P. $P < 0$ refers to substrates placed on the powered electrode.

n values) with low concentrations of voids and other defects are produced in the low-P (low-D) regime, substrates being placed on the grounded electrode.

Raman Spectroscopy

Micro-Raman spectroscopy (MRS) is a non-destructive optical technique that can be used to analyze structural
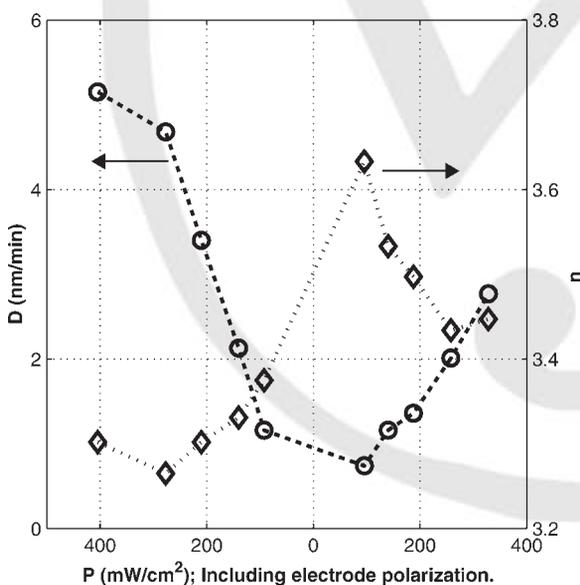

Figure 4. Influence of power density, P, on deposition rate, D, and refractive index, n, of a-Si:H films, deposited on glass at $T_s = 27\,°C$. $P < 0$ refers to substrates placed on the powered electrode.
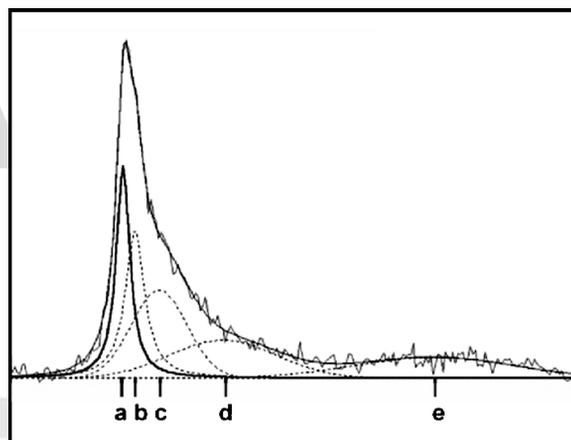

Figure 5. Example of a Si-Si micro-Raman spectrum, corresponding to an nc-Si:H film deposited on PA at $T_s = 175\,°C$ (see Table 2 for description).

properties of semiconductors.[6,11–17] In silicon, the transverse optical (TO) vibration modes differ between c-Si and a-Si:H materials. Within a multiphase material, for example nc-Si:H, we can estimate the crystalline volume fraction, X_c, by comparing the contributions from the "c" and "a" peaks. Further information can also be derived from the center frequency positions, ω, and the full widths at half-maximum (FWHM), Γ, of the peaks, as will be discussed below. X_c can be estimated using the formula:[11]

$$X_c = \frac{I_c + I_{gb}}{I_c + I_{gb} + y(L)I_a} \qquad (3)$$

where I_c, I_{gb}, and I_a are the integrated intensities of (or areas under) the "crystalline", intermediate (grain boundary), and "amorphous" peaks, respectively (see Figure 5 and Table 2). The weighting function, $y(L)$, is the ratio of the scattering cross-section of c-Si to a-Si:H, which depends on the excitation wavelength, λ, and the grain size, L; according to Bustarret et al.,[11] $y(L) = 0.1 + \exp(-L/250)$; in other words, y is close to unity, $0.9 < y(L) < 1.1$ for the case of small grain sizes ($0 < L < 20$ nm). Since the deposition conditions used here are known to lead to L values < 20 nm,[5–7] we have used $y = 1$ in our calculations,

Table 2. Data analysis of the micro-Raman spectrum shown in Figure 5.

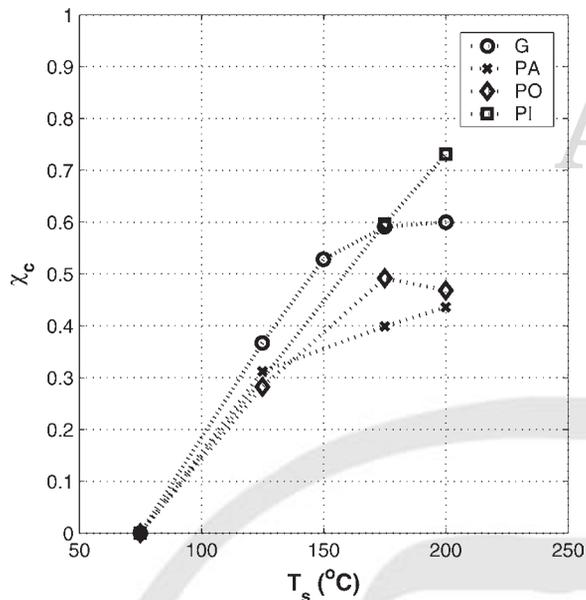| Symbol	ω_0	Γ	Peak assignment	Reference
	cm^{-1}	cm^{-1}		
a	520	4–15	c-Si TO	[6,11–17]
b	494–510	20–30	gb-Si	[6,12,13]
c	480	45–80	a-Si:H TO	[6,11–17]
d	440	≈100	a-Si:H LO	[17]
e	330	≈120	a-Si:H LA	[17]

Figure 6[Q1]. The influence of T_s on the crystalline volume fraction, X_c, estimated using Equation (3), for different substrate materials.

the results of which appear in Figure 6. Figure 6 represents a plot of X_c vs. T_s: films are seen to be essentially amorphous ($X_c \approx 0$) for $T_s < 100\,°C$, but the crystalline fraction, X_c, then rises near-linearly with increasing T_s values. The majority of our nc-Si:H films, corresponding to deposits made at $150\,°C \leq T_s \leq 225\,°C$, show a maximum X_c of ≈ 0.5. Increasing either T_s or the deposition duration (film thickness) resulted in unstable film-substrate composite structures, as will be discussed later.

The measured peak-center positions, ω, and FWHM, Γ, of our a-Si:H and nc-Si:H samples vary considerably, depending on the chosen substrate material and T_s. For the c-TO peak $\omega = 516 \pm 4\ \text{cm}^{-1}$ and $\Gamma = 13 \pm 3\ \text{cm}^{-1}$, while for the a-TO peak $\omega = 485 \pm 10\ \text{cm}^{-1}$ and $\Gamma = 55 \pm 10\ \text{cm}^{-1}$. Onset of the intermediate peak (Table 2, symbol b) coincided with that of the crystalline peak; its ω and Γ values were $\omega = 503 \pm 4\ \text{cm}^{-1}$ and $\Gamma = 25 \pm 5\ \text{cm}^{-1}$. A full examination of this data will not be presented here due to the many film properties and measurement conditions that can affect ω and Γ. Some of these factors include: (i) the size and shape of crystallites,[14] (ii) the local temperature of the measured volume, T_m,[15] which can be raised by the probe laser, and (iii) residual stresses (both intrinsic and extrinsic) which are variable throughout the film thickness.[16]

DC Conductivity

The electrical conductivity of semiconducting materials such as nc-Si:H, $\sigma(T)$, is thermally activated and therefore

obeys the Arrhenius relation:

$$\sigma(T) = \sigma_0 \exp\left(\frac{-E_a}{kT}\right) \tag{4}$$

where σ_0 is the pre-exponential factor, E_a is the so-called activation energy, and k is Boltzmann's constant. For the case of nc-Si:H films grown directly on plastic substrates, the temperature dependence of $\sigma(T)$ is also influenced by stress in the film resulting from the differential thermal expansion between it and the substrate.[8−10] After repeated thermal cycles, excessive stresses may result in failure (cracking and delamination of the nc-Si:H) of the f-s composite. Figure 7 and 8 present $\sigma(T)$ data for nc-Si:H films on PA and PO substrates, respectively, measured while continuously heating and cooling the composites ($dT/dt = 0.33\,°C/min$) within a range of temperatures, $40\,°C < T < 120\,°C$. "Good" f-s composite structures display the expected near-linear behavior (Figure 7), while a highly non-linear behaviour is observed for the case of nc-Si:H/PO (Figure 8). Values of σ and E_a for "good" nc-Si:H films grown at particular fixed conditions were always found to be very similar, independent of whether they were deposited on polymers or on glass. "Arrhenius-like" behavior within the specified T range was observed for all films deposited at $T_s \leq 175\,°C$, except for those grown on the PO substrate. The reason for this "anomaly" is the following: As shown in Figure 2, APPEAR® (PO) undergoes a structural transition at $T \approx 60\,°C$ that gives rise to increasing $\alpha(T)$ values above that temperature. As a result,
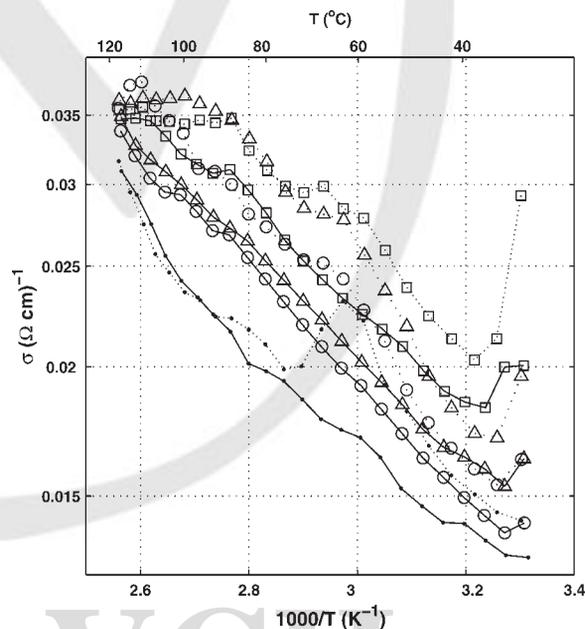

Figure 7. $\sigma(T)$ values for nc-Si:H films deposited at $T_s = 175\,°C$ on PA, during four cycles within the temperature range: ($40\,°C < T < 120\,°C$).
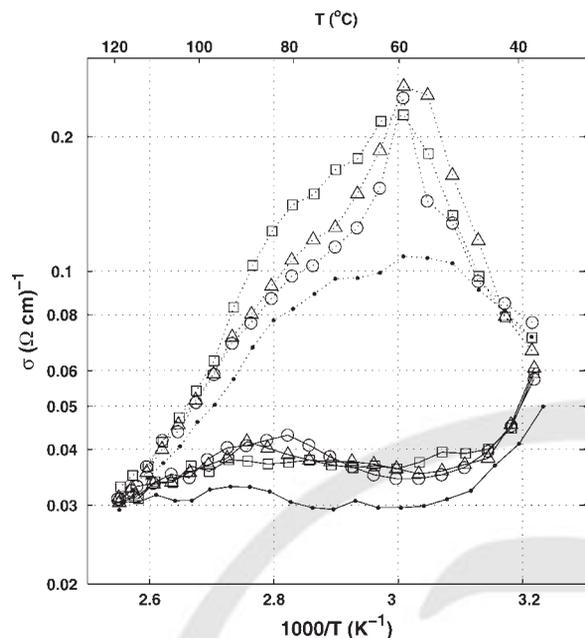
Figure 8. $\sigma(T)$ values for nc-Si:H films deposited at $T_s = 175\,°C$ on PO, during four cycles through the temperature range: $(40\,°C < T < 120\,°C)$.

Figure 9. Arrhenius plots for nc-Si:H films on glass and on three polymer substrates, all deposited at $T_s = 175\,°C$.

stress values in the nc-Si:H deposits on this substrate increase concomitantly with rising T, and this gives rise to the hysteretic, non-Arrhenius behavior observed in Figure 8. For the case of all other substrate materials, α is either constant or only mildly T-dependent (see Figure 2 and Table 1) so that this "anomaly" does not occur. The series of near-parallel linear curves in Figure 7, which eventually stabilize to a single, reproducible one, result from gradual relaxation of the residual stresses in the polymer that originate from the manufacturing process.

In Figure 9 we present a series of Arrhenius plots corresponding to different substrate materials (PS, PA, PI and glass), in all cases following mechanical relaxation of possible stresses in the substrates, and all nc-Si:H films having been deposited under identical conditions at $T_s = 175\,°C$. Clearly, the curves are all parallel ($E_a = 92 \pm 5$ meV), but the $\sigma(T')$ values can differ by a factor of about 1.5 for any given T' value. For easier comparison with data from the literature, we shall focus our attention on our data pertaining to the Corning 2947 glass substrate material: Figure 10 shows plots of $\sigma(300\ K)$, values measured at 300 K, versus the corresponding apparent E_a values, along with similar plots drawn from the literature.[7,20] Even though the latter correspond to significantly different fabrication conditions (for example, Ram et al.[7] used SiF_4 as their Si feed gas, instead of SiH_4), the three data sets are remarkably similar. Figure 11 and 12 show plots of $\sigma(300\ K)$ and of E_a values versus T_s and X_c, respectively, for the present a-Si:H and nc-Si:H deposits, again on the Corning 2947 glass substrates. Like the data displayed in Figure 10, these illustrate the remarkable range of property variations,
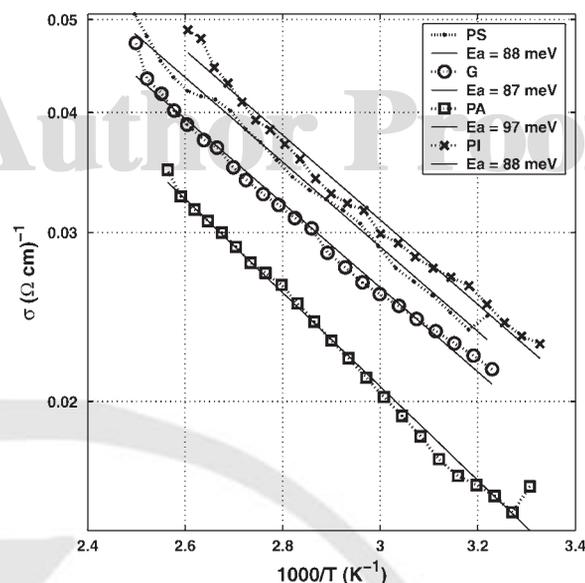
their systematic dependence on T_s (or X_c, itself strongly dependent on T_s), and their excellent reproducibilities achieved in the current research. Although the data are not shown here (other than in the example of Figure 9), similar results were also obtained with the "well-behaved" polymer substrates, that is, all but PO.

As mentioned in connection with Figure 10, the present data correlate well with those in the literature, but only if one takes into account the "normal" existence of oxygen doping of the nc-Si:H at the ppm level. This is
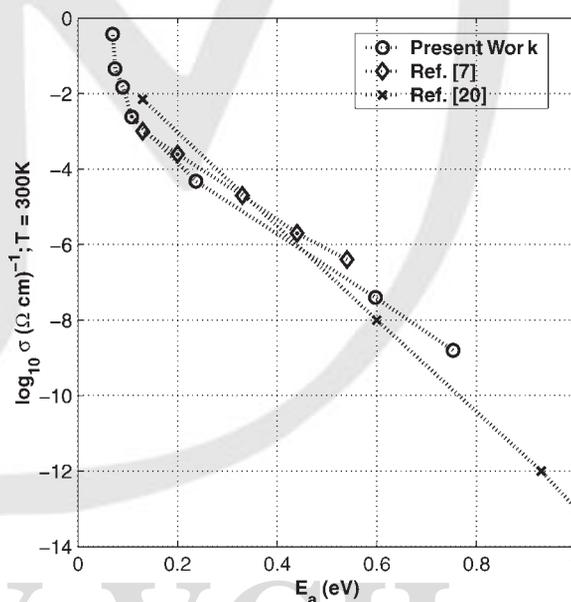

Figure 10. Plots of σ values measured at 300 K versus the corresponding apparent E_a values, for the present work and data from the literature.[7,20]
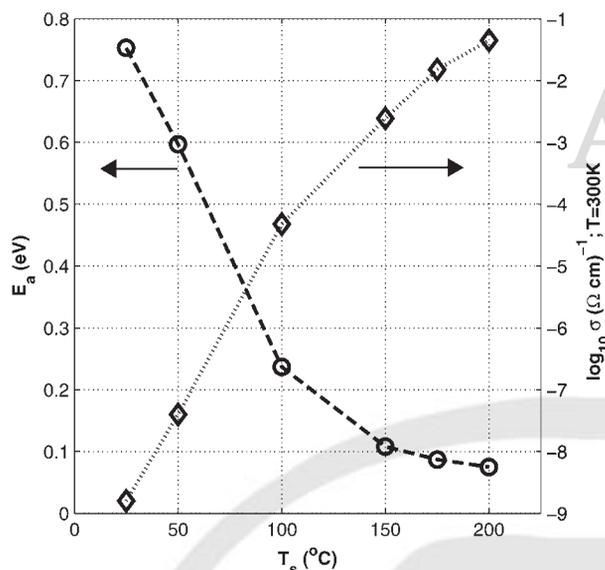
Figure 11. Plots of $\sigma(300\ K)$ and of E_a values versus substrate temperature, T_s, at which the nc-Si:H films were deposited, for the case of Corning 2947 glass substrate material.

known to occur on account of trace quantities of O_2 and H_2O in the reactor; Torres et al.[21] demonstrated that O-doping could only be avoided by taking extraordinary measures for assuring purity of the feed gas and of the reactor system.

General Discussion and Conclusion

Like the present work, other earlier research[5−7] also had an objective to elucidate the structural evolution of thin Si
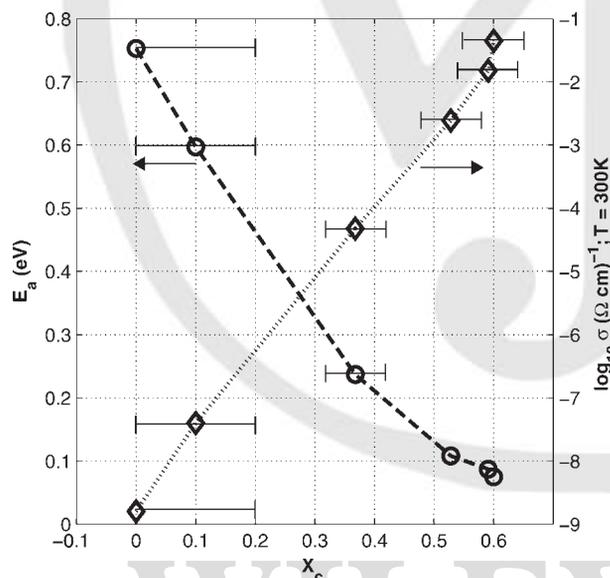

Figure 12. Plots of $\sigma(300\ K)$ and of E_a values versus the films' crystalline volume fraction, X_c, for the case of nc-Si:H films deposited on Corning 2947 glass.

films, deposited by PECVD from SiH_4 mixtures highly diluted in H_2, for the most part using silica or c-Si substrates. With a suitable choice of C_{SiH_4} (between 5% and 8%, 6.25% in the present case) it was found that the nanostructure of deposited films can be effectively controlled by varying a single parameter, T_s.[5−7] The present structural and electrical results also clearly demonstrate that a very wide range of material properties can be achieved simply by varying T_s within the range tolerated by the current substrate materials ($T_s < 250\ ^\circ C$). The first appearance of nanocrystalline structure (detected by MRS) occurred at $T_s = 100 \pm 10\ ^\circ C$ (Figure 6). Thermal expansion of these substrates has clearly been our greatest challenge for the development of highly stable film-substrate composite structures. Compressive strains ($\alpha_s \Delta T \approx 1.7\%$) and compressive stress values $s_f \approx 3.6$ GPa, have been identified as those that clearly exceeded the adhesive strength of the nc-Si:H/PO interface, when $T_s \geq 200\ ^\circ C$. Although highly stressed samples (PO substrate, $T_s = 175\ ^\circ C$) were not observed to immediately delaminate, their $\sigma(T)$ behavior was hysteretic (Figure 8), and they eventually did delaminate after numerous thermal cycles ($\approx$10 cycles of $\approx$8 h per cycle). The large majority of nc-Si:H films on polymers nevertheless showed resilience, as evidenced by the stability of their electrical behaviors (linear Arrhenius plots for nc-Si:H on all substrates other than PO), even when repeatedly subjected to $\approx$GPa stresses, both in tension and compression, for example during continuous thermal cycling for periods in excess of 80 h. Like Angiolini et al.,[1] we are therefore confident that the results presented here "point to the successful fabrication of high-performance TFT arrays on plastic substrates".

The high-T_g polymers we have used here as substrates fulfill certain important requirements for electronic applications, for example in OLED technology: Their high T_g values and their resistance to plasma-induced ablation have allowed us to deposit satisfactory nc-Si:H layers by RF-PECVD, subject to the selection of suitable deposition parameters. The high expansion coefficients of some polymers, particularly of PO, remains an important obstacle opposing fabrication of reliable devices, yet the resilience of nc-Si:H films observed on substrates other than PO is encouraging. Relationships between deposition conditions, structural and transport properties that we have observed manifest much similarity between the behaviors of nc-Si:H films grown on glass and on polymer substrates.

[1] S. Angiolini, M. Avidano, R. Bracco, C. Barlocco, N. D. Young, M. Trainor, X.-M. Zhao, *SID Digest* **2003**, 47.1.

[2] Anon, ''see what can be high performance films''; pamphlet published jointly by Ferrania Imaging Technologies, Promerus LLC and Sumitomo Bakelite Co., Ltd.

[3] ''*Thin Film Transistors*'', Y. Kuo, Ed., Kluwer Academic Publishers, Dordrecht 2004.

[4] *SOI Design: Analog, Memory and Digital Techniques*, A. Marshall, S. Natarajan, Eds., Kluwer Academic Publishers, Dordrecht 2002.

[5] U. Kroll, J. Meier, A. Shah, S. Mikhailov, J. Weber, *J. Appl. Phys.* **1996**, *80*, 4971.

[6] O. Vetterl, A. Gross, T. Jana, S. Ray, A. Lambertz, R. Carius, F. Finger, *J. Non-Cryst. Sol.* **2003**, *299–302*, 772.

[7] S. K. Ram, S. Kumar, R. Vanderhagen, P. Roca, I. Cabarrocas, *J. Non-Cryst. Sol.* **2002**, *299–302*, 411.

[8] Z. Suo, E. Y. Ma, H. Gleskova, S. Wagner, *Appl. Phys. Lett.* **1999**, *74*, 1177.

[9] H. Gleskova, S. Wagner, Z. Suo, *Appl. Phys. Lett.* **1999**, *75*, 3011.

[10] M. Ohring, ''*Material Science of Thin Films*'', 2nd edition, Academic Press, Boca Raton 2002.

[11] E. Bustarret, M. A. Hachicha, M. Brunel, *Appl. Phys. Lett.* **1988**, *52*, 1675.

[12] G. Yue, J. D. Lorentzen, J. Lin, D. Han, Q. Wang, *Appl. Phys. Lett.* **1999**, *75*, 492.

[13] C. Droz, E. Vallet-Sauvain, J. Bailat, L. Feitknecht, J. Meier, A. Shah, *Solar Energy Mater. Solar Cells* **2004**, *81*, 61.

[14] I. H. Cambell, P. M. Fauchet, *Solid State Commun.* **1986**, *58*, 739.

[15] D. M. Bhusari, A. S. Kumbhar, S. T. Kshirsagar, *Phys. Rev. B* **1993**, *47*, 6460.

[16] V. Paillard, P. Puech, P. Roca, I. Cabarrocas, *J. Non-Cryst. Sol.* **2002**, *299–302*, 280.

[17] J. Owen, D. Han, B. Yan, J. Yang, K. Lord, S. Guha, *NCPV and Solar Review Meeting*, 2003, NREL/CD-520-33586, 776.

[18] F. M. Smits, *Bell Syst. Tech. J.* **1958**, 37.3.

[19] D. M. Manos, D. L. Flamm, ''*Plasma Etching: An Introduction*'', Academic Press, Boston 1988.

[20] R. Platz, S. Wagner, *J. Vac. Sci. Technol. A* **1988**, *16*, 3218.

[21] P. Torres, J. Meier, R. Fluckinger, U. Kroll, J. A. Anna Selvan, H. Keppner, A. Shah, S. D. Littelwood, I. E. Kelly, P. Giannoules, *Appl. Phys. Lett.* **1996**, *69*, 1373.

Q1: Please check Figure 6, 7, and 8, e-file and hardcopy mismatch.